Author Manuscript

Author Manuscript

Author Manuscript

Author Manuscript

HHS Public Access

Author manuscript

Head Neck. Author manuscript; available in PMC 2019 August 01.

Published in final edited form as:

Head Neck. 2016 August ; 38(8): 1176–1186. doi:10.1002/hed.24269.

Pools of programmed death-ligand within the oral cavity tumor microenvironment: Variable alteration by targeted therapies

Sujay Shah, MD[1], **Andria Caruso, MD**[2], **Harrison Cash, BS**[1], **Carter Van Waes, MD, PhD**[1], **Clint T. Allen, MD**[1,3,*]

[1]Tumor Biology Section, Head and Neck Surgery Branch, National Institutes of Deafness and Other Communication Disorders, National Institutes of Health, Bethesda, Maryland, [2]Department of Otolaryngology–Head and Neck Surgery, Walter Reed National Military Medical Center, Bethesda, Maryland, [3]Department of Otolaryngology – Head and Neck Surgery, Johns Hopkins School of Medicine, Baltimore, Maryland.

Abstract

Background.—Enhanced understanding of programmed death-ligand (PD-L) expression in oral cancer is important for establishing rational combinations of emerging immune checkpoint and molecular targeted therapies.

Methods.—We assessed PD-L and interferon (IFN) expression in immunogenic murine oral cancer-1 (MOC1) and poorly immunogenic MOC2 cell models after treatment with mammalian target of rapamycin (mTOR) and MEK1/2 small molecule inhibitors in vitro and in vivo.

Results.—PD-L1 but not PD-L2 is expressed on MOC1 and 2 cells and is type I and II IFN-dependent. PD-L1 is differentially expressed on cancer and endothelial cells and infiltrating myeloid-derived suppressor cells, macrophages, and regulatory T cells (Tregs) in highly and poorly immunogenic tumors. PD-L1 expression is variably altered after treatment with inhibitors in vivo, with an imperfect relationship to alterations in IFN levels in the tumor microenvironment.

Conclusion.—PD-L1 expressed on cancer and infiltrating immune cells is variably altered by targeted therapies and may, in part, reflect changes in tumor IFN. © 2016 Wiley Periodicals, Inc. *Head Neck* 38: 1176–1186, 2016

Keywords

programmed death; oral cancer; targeted therapy; interferon

[*]Corresponding author: C. T. Allen, Tumor Biology Section, Head and Neck Surgery Branch, National Institutes of Deafness and Other Communication Disorders, National Institutes of Health, 10 Center Drive, CRC 4-2740, Bethesda, MD 20892. allen.clint@nih.gov.

This work was presented in part at the 2015 American Head and Neck Society Translational Research Conference in Boston, MA, April 22–23, 2015.

Author Manuscript Author Manuscript Author Manuscript Author Manuscript

INTRODUCTION

Many human cancers demonstrate deregulated cytokine and chemokine expression and lack infiltration of innate and adaptive immune cells indicative of immunologic exclusion.[1] Other tumors demonstrate evidence of significant local inflammatory and immune responses indicative of a T-cell inflamed status, yet, by definition, have escaped immune elimination. Ligation of programmed death (PD-1) receptors on effector T cells by programmed death-ligands (PD-Ls)-1 and 2 (PD-L1/2) expressed on tumor, immune, and stromal cells within the tumor microenvironment seems to be one mechanism of immune escape in these tumors.[2–4] Significant proportions of both carcinogen-associated and human papillomavirus-associated head and neck squamous cell carcinomas (HNSCCs) demonstrate a T-cell inflamed gene expression and immune infiltration profile along with tumor cell PD-L1/2 expression.[5–7] Yet, only a subset of patients achieve durable antitumor responses with either PD-1 or PD-L1 monoclonal antibody (mAb) therapy,[8,9] even in the patient population with HNSCC enriched for tumor microenvironment PD-L1 expression.[6] Intrinsic tumor cell expression of PD-L1/2 downstream of oncogenic signaling pathways, as opposed to reactive tumor cell PD-L expression in response to an inflammatory, interferon (IFN)-rich microenvironment, may represent one mechanism of resistance.[10] Thus, combining small molecule inhibitors that target oncogenic pathways with PD-blocking mAbs is an attractive approach to enhance the proportion of patients that respond to these immunotherapies.

The Cancer Genome Atlas integrated genomic analysis demonstrates frequent mutations and copy number alterations in receptor and signaling kinases that lead directly to the activation of the phosphoinositide 3-kinase/mechanistic target of rapamycin (PI3K/mTOR) pathway in both carcinogen-associated and human papillomavirus-associated HNSCCs.[11] Although upstream Ras mutations are rare events in HNSCC, the mitogen-activated protein kinase (MAPK)/extracellular signal-related kinase is often coactivated in HNSCC because of growth factor receptor activation and crosstalk between the PI3K/mTOR pathway.[12] For these reasons, small molecule inhibitors that target these pathways are the subject of current investigation for HNSCC, yet, little is known about the contribution of these pathways to PD-L1/2 expression on cancer cells. Furthermore, the effects that such systemic targeted therapies may exert on tumor stromal or infiltrating immune cell PD-L1/2 expression is poorly characterized.

The murine oral cancer (MOC) models consist of cell lines with variable in vivo aggressiveness and metastatic potential.[13] MOC1-generated tumors are slow growing, do not metastasize, demonstrate a robust CD81 T-cell infiltrate, and are highly immunogenic, whereas MOC2-generated tumors grow rapidly, metastasize to draining lymph nodes early, demonstrate an immunosuppressive hematopoietic infiltrate, and are poorly immunogenic.[14,15] These models allow the study of antitumor immune responses and alterations of the tumor microenvironment in both T-cell inflamed and non–T-cell inflamed tumors in immune-competent mice.

In this study, we utilized these models of oral cavity cancer to characterize mechanisms of PD-L1/2 expression on tumor cells in vitro. We next assessed baseline pools of PD-L1/2 expression in vivo in the tumor microenvironment of both highly immunogenic MOC1 and

Author Manuscript Author Manuscript Author Manuscript Author Manuscript

poorly immunogenic MOC2 tumors. Further, we evaluated how pharmacologic inhibition of mTOR with rapamycin and mitogen-activated protein kinase (MEK) with PD0325901 (PD901) treatment-altered PD-L1/2 expression on tumor and mesenchymal cell subsets and IFN levels within the tumor microenvironment.

MATERIALS AND METHODS

Cells, cell culture, and in vitro treatments

Carcinogen-induced MOC cells were generated, as described previously.[13] MOC cells were cultured in Iscove's modified Dulbecco medium/F12 at a 2:1 mixture with 5% fetal calf serum (FCS; Fischer Scientific, Houston, TX), 1% penicillin/streptomycin, 5 ng/mL epidermal growth factor (EGF; Millipore, Billerica, MA), 400 ng/mL hydrocortisone, and 5 ng/mL insulin (Sigma, St. Louis, MO). Cells were incubated at 37°C with 5% CO_2. FCS, EGF, and insulin were removed from media for certain experiments where indicated. Stimulation of MOC cells with murine cytokines (R&D, Minneapolis, MN), as indicated, was performed for 48 hours after 24 hours of serum starvation. Treatment of MOC cells with pharmaceutical grade rapamycin (LC Laboratory, Woburn, MA) and PD901 (SelleckChem, Houston, TX) was performed for 48 hours in complete media as above.

Mice and in vivo treatments

Experiments were carried out using 8 to 10-week-old female C57BL/6 mice purchased from the National Cancer Institute Animal Production Facility in Frederick, MD. All animal studies were approved by the National Institute of Deafness and Other Communication Disorders Animal Care and Use Committee (ASP1364–14). To generate tumors, 1×10^6 MOC1 or 1×10^5 MOC2 cells were transplanted subcutaneously in the right flank. Tumors were allowed to engraft and reach a size of 0.1 cm^3 (6–7 mm diameter; 30 days for MOC1 and 14 days for MOC2) before being treated. Mice treated with rapamycin received a loading dose of 4.5 mg/kg via intraperitoneal (i.p.) injection, followed by 1.5 mg/kg via i.p. injection every other day for 21 days. Mice treated with PD901 received 1.5 mg/kg via oral gavage (OG) daily for 21 days. In vivo doses of drugs were determined both from published rodent pharmacokinetic data to match human serum drug concentrations[16,17] and from our laboratory's experience with lack of animal toxicity with these drug doses in murine xenograft models. Control mice were treated with drug carriers alone administered via i.p. injection and OG. After 21 days of therapy, treated and control tumor-bearing mice were euthanized and tumors were surgically removed. Tumor tissue used for real-time polymerase chain reaction (RT-PCR) was snap frozen and stored at −80°C until use, tissue used for immunohistochemistry was embedded in optimum cutting temperature media (Fischer Scientific) and stored at −80°C until use, and tissue for flow cytometric analysis was used fresh on the same day as tumor harvest.

Flow cytometry

After in vitro stimulation or treatment as indicated, MOC cells were harvested using a cell scraper, gently pipetted, and passed through a 40 μM filter to generate a single cell suspension. Nonspecific binding was blocked using an anti-mouse CD16/32 antibody (Biolegend, San Diego, CA) and cells were stained with fluorophore conjugated anti-mouse

Author Manuscript Author Manuscript Author Manuscript Author Manuscript

PD-L1 clone 10F.9G2 (Biolegend) and PD-L2 clone TY25 in a 1% bovine serum albumin/1 × phosphate-buffered saline buffer. After in vivo treatment as indicated, fresh tumor tissue was minced into 1-mm pieces and digested into a single suspension using the murine tumor dissociation kit from Miltenyi Biotech (Auburn, CA) per protocol. Both chemical and mechanical (gentleMACS, Miltenyi) dissociation techniques were utilized with consistent cell viability of 70% or greater. After filtering the tumor suspension, cell surface staining was performed using fluorophore conjugated anti-mouse CD45.2 clone 104, CD140a clone APA5, CD31 clone 390, Gr1 clone RB6–8C5, Cd11b clone M1/70, Ly6C clone HK1.4, F4/80 clone BM8, PD-L1 clone 10F.9G2, and PD-L2 clone TY25 (Biolegend) as indicated. Intracellular staining for FoxP3 in CD4+ T-lymphocytes to identify regulatory T cells (Tregs) was performed using the eBioscience (San Diego, CA) Treg staining kit per protocol. Specific staining of each antibody used was validated with the use of isotype control antibodies and a “fluorescence minus one” method of antibody combination validation. Specific staining of the PD-L2 antibody clone TY25 was further validated with positive macrophage staining in other experimental conditions (data not shown). For all stains, viable cells were gated via 7AAD negativity. Data were acquired on a FACSCanto using FACSDiva software (BD Biosciences, San Diego, CA) and analyzed on FlowJo software (Ashland, OR).

Polymerase chain reaction

Tumor lysates were generated using the Tissue Lyser II (Qiagen) and total RNA was purified using the RNeasy Mini Kit (Qiagen), in accord with the manufacturer’s instructions. Yields and quality were assessed by Nano-drop 2000 (Thermo Scientific) and concentrations of each sample were adjusted to the same levels before cDNA synthesis. cDNA was then synthesized utilizing the High Capacity cDNA Reverse Transcription Kit (Clontech) and mRNA expression was analyzed by RT-PCR. Taqman Single Tube primers for IFNβ and IFNγ and Taqman Universal PCR Master Mix (Life Technologies) were used in combination to assess the relative expression of target genes in comparison to a glyceraldehyde 3-phosphate dehydrogenase housekeeping gene on a Viia7 quantitative PCR machine (Applied Biosystems).

Immunohistochemistry

Optimum cutting temperature-embedded tumors were sectioned (Histoserv, Germantown, MD). Sections of 6-μM thickness were fixed via immersion in ice-cold acetone before serum block and staining with anti-mouse PD-L1 (clone 10F.9G2) or isotype control antibody (BioLegend). Signal was amplified with ABC peroxidase and slides were stained with diaminobenzidine (Vector Labs, Burlingame, CA) per protocol. Stained samples were washed before nuclear counterstaining with Hematoxylin QS (Vector Laboratories) and mounted with Permount (Fisher Scientific). Whole slides were digitized for analysis using the Aperio ScanScope CS system. Eight, 40× high-powered fields were analyzed from each sample with exclusion of necrotic regions.

Statistical analysis

Tests of significance between pairs of data are reported as p values, derived using a t test with a 2-tailed distribution, and calculated at 95% confidence intervals. Comparison of

Author Manuscript Author Manuscript Author Manuscript Author Manuscript

multiple sets of data was achieved with 1-way or 2-way analysis of variance. Significance was set in each case to $p < .05$. Calculations were performed using GraphPad Prism version 6.0 for Macintosh.

RESULTS

Programmed death-ligand expression on murine oral cancer cells is dominantly influenced by interferon

Many HNSCC tumors express PD-L1/2,[6] yet, the relative contribution of intrinsic and extrinsic signals inducing their expression is poorly defined. We assessed baseline PD-L expression in MOC1 and MOC2 cells in vitro using flow cytometric analysis. PD-L1 but not PD-L2 was expressed on a subset of cells at baseline in serum-starved MOC cells, with MOC2 having higher baseline PD-L1 expression than MOC1 in vitro (mean fluorescence intensity [MFI] 135 ± 13 vs 93 ± 6, respectively; $p < .01$). To assess the individual contribution of different cytokines and growth factors found in the HNSCC tumor microenvironment to PD-L expression, different mitogenic stimuli and proinflammatory cytokines were individually added to MOC cells. IFNβ and IFNγ both significantly induced expression of PD-L1 in both MOC1 and MOC2 cells (both $p < .001$; Figure 1A). The addition of standard mitogenic stimuli (FCS, EGF, and insulin, indicated as complete media in Figure 1A), interleukin-1α (IL-1α), IL-6, tumor necrosis factor-α, or transforming growth factor-β failed to induce expression of PD-L1. PD-L2 expression was not induced with any condition tested (Figure 1B).

To evaluate the contribution of mTOR or MEK signaling to baseline PD-L1 expression in vitro, MOC1 and MOC2 cells were exposed to pharmacologic inhibitors. The mTOR inhibitor rapamycin, at a dose that suppresses phosphorylation of the downstream target S6-kinase (results not published), did not alter PD-L1 expression in MOC1 or MOC2 cells (Figure 1C). Conversely, the MEK1/2 inhibitor PD0235901 (PD901), given at a dose that potently inhibits phosphorylation of downstream extracellular signal-related kinase 1/2 (results not published), modestly but significantly increased PD-L1 expression alone in MOC1 ($p < .05$) or in combination with rapamycin in MOC2 ($p < .05$). We then assessed the effect of pharmacologic inhibition of mTOR or MEK on IFN-inducible PD-L1 expression. With the exception of a reduction in IFNβ-induced PD-L1 expression after rapamycin treatment in MOC1, either the targeted drug alone or in combination potentiated IFNβ-induced or IFNγ-induced PD-L1 expression in both cell lines. Taken together, these data indicate that PD-L1 expression on MOC tumor cells is highly responsive to the presence of extracellular type I (IFNβ) or type II (IFNγ) interferon and that small molecule inhibitors targeting mTOR and MAPK signaling do not abrogate baseline or IFN-responsive PD-L1 expression.

Baseline PD-L expression in MOC tumor and host cell subsets is diverse and imperfectly correlates with in vivo IFN levels

We wished to assess baseline PD-L expression in different pools of cells within the complex tumor microenvironment. To accomplish this, we first generated single cell suspensions from MOC1 and MOC2-generated tumors in immunocompetent mice and performed flow

Author Manuscript Author Manuscript Author Manuscript Author Manuscript

cytometry using cell surface makers to identify individual cell types. In both MOC1 and MOC2 tumors, PD-L1 but not PD-L2 was expressed on CD45(−)/CD31(−) tumor cells as well as on CD31(+)/CD45(−) tumor endothelial cells and CD45(+)/CD31(−) infiltrating immune cells (Figure 2). Cancer-associated fibroblasts, identified with a platelet-derived growth factor receptor (CD140a) specific antibody, were rare (<5% of CD45(−)/CD31(−) cells) and expressed low levels of PD-L1 (data not shown). Complementing the in vitro findings, PD-L1 is the dominant PD-L expressed and is the same on multiple different epithelial and infiltrating immune cell types in vivo.

The relative expression of PD-L1 in different pools of cells in both MOC1 and MOC2 tumors was quantified. Slow-growing, immunogenic MOC1 tumors are composed of tumor and infiltrating CD45(+) cells, whereas MOC2 tumors are highly vascular with more robust CD45(−)/CD31(+) cell infiltration (Table 1). Although PD-L1 was expressed on tumor and vascular cells in both tumors, the number of positive cells and levels of PD-L1 expression were significantly higher in MOC1 tumors. Whereas both tumors harbor a similar degree of hematopoietic cell infiltration, immune cell infiltration in MOC2 is composed primarily of immature, highly inflammatory myeloid-derived suppressor cells and significantly more FoxP3(+) Tregs compared to MOC1. Similar to tumor and endothelial cells, surface PD-L1 expression was higher on myeloid-derived suppressor cells in MOC1 tumors.[14] Because the majority of the myeloid infiltrate into MOC2 tumors is immature, there are significantly less F4/80(+) mature macrophages, yet the PD-L1 expression on these MOC2 macrophages was dramatically higher compared to MOC1. There was no significant difference in Treg PD-L1 expression between the 2 tumors. These data indicate that PD-L1 is diffusely expressed on a wide range of cell types within the MOC tumor microenvironment. Interestingly, PD-L1 expression is consistently higher on cell subsets of MOC1 tumors, with the exception of significantly higher PD-L1 expression on MOC2 tumor infiltrating macrophages.

To validate our flow cytometric PD-L1 expression findings, we visualized PD-L1 levels in untreated MOC1 and MOC2 tumors by immunohistochemistry. Staining with the same antibody clone that was used for flow cytometry revealed membranous PD-L1 expression on approximately 15% to 20% of MOC1 tumor cells. This baseline MOC1 PD-L1 expression level was significantly higher than MOC2, consistent with our flow data.

Given that PD-L1 expression on MOC1 and MOC2 cells in vitro is highly responsive to IFN, we hypothesized that IFN levels in vivo would correlate with relative PD-L1 expression in MOC1 and MOC2 tumors (Figure 3B). Using PCR, we evaluated relative baseline transcript levels of IFNβ and IFNγ in fresh MOC1 and MOC2 tumor tissue. MOC1 tumors expressed significantly more IFNγ than IFNβ and 114-fold more IFNγ than MOC2 tumors. Surprisingly, MOC2 tumors expressed significantly more IFNβ than IFNγ and 12-fold more IFNβ than MOC1 tumors. Higher baseline IFNγ levels in MOC1 tumors along with higher baseline PD-L1 expression on tumor cells, endothelial cells, and tumor infiltrating myeloid-derived suppressor cells is consistent with adaptive immune resistance, linking PD-L1 expression to IFNγ levels in tumors.[4] Conversely, the significantly elevated PD-L1 expression on MOC2 infiltrating macrophages and the lack of difference on infiltrating Tregs suggests these cells may have IFNβ-dependent or undefined IFN-independent PD-L1 expression.

Author Manuscript Author Manuscript Author Manuscript Author Manuscript

Programmed death-ligand-1 expression is variably altered in tumors after targeted therapy

MOC1 and MOC2 tumor-bearing mice were treated with rapamycin and PD901 alone or in combination for 21 days and tumors were evaluated for PD-L1 expression. Changes in PD-L1 surface expression differed based on cell type and tumor microenvironment (Figure 4). In immunogenic, IFNγ-high MOC1 tumors, cancer cell and tumor-infiltrating macrophage PD-L1 expression was significantly decreased with combination mTOR and MEK inhibition with a trend toward reduced PD-L1 expression with either drug alone (Figures 4A and 4D). However, PD-L1 expression on other MOC1 cell subsets was not significantly altered (Figures 4B, 4C, and 4E). In poorly immunogenic, IFNγ-low MOC2 tumors, MEK inhibition reduced PD-L1 expression alone or in combination with mTOR inhibition on cancer cells and infiltrating myeloid-derived suppressor cells, macrophages, and Tregs (Figures 4A, 4C–4E). Because of low baseline expression of PD-L1 on MOC2 tumor cells, the reduction in PD-L1 expression is small compared to that seen on MOC1 tumor cells, but remains statistically significant. Remarkably, MEK inhibition alone or in combination with mTOR inhibition increased PD-L1 expression on MOC2 CD45(−)/CD31(+) endothelial cells (Figure 4B). These data indicate a notable difference in regulation of PD-L1 expression in response to MEK inhibition between MOC1 and MOC2 tumors. Although MEK blockade reduced PD-L1 expression in both MOC1 and MOC2 tumor cells, it variably altered PD-L1 expression in MOC1 and MOC2 endothelial cells and tumor-infiltrating myeloid-derived suppressor cells, macrophages, and Tregs.

Changes in tumor interferon levels after targeted therapy differentially correlate with altered programmed death-ligand-1 expression in murine oral cancer-1 and murine oral cancer-2 tumors

After treatment with rapamycin and PD901, tumor IFNβ and IFNγ transcript levels were measured (Figure 5). In MOC1 tumors, high baseline IFNγ expression was significantly suppressed after MEK inhibition alone or in combination with mTOR inhibition, suggesting a degree of immune suppression. MEK inhibition alone induced IFNβ expression in MOC1 tumors, but low baseline expression makes this change of unclear significance. Reduced IFNγ in MOC1 tumors after MEK inhibition correlates with decreased PD-L1 expression on MOC1 tumor cells and infiltrating macrophages, suggesting an IFN-dependent mechanism of PD-L1 expression in these but no other cells in the MOC1 tumor microenvironment. IFNγ transcript levels were significantly reduced after MEK and mTOR inhibition alone or in combination in MOC2 tumors, but low baseline levels of this cytokine makes the significance of this finding unclear as well. Similar to IFNγ, IFNβ was reduced by both MEK and mTOR inhibition alone or in combination, and may have played a role in regulation of PD-L1 expression in cells that were altered in MOC2 but not MOC1. Overall, whereas these reduced IFN levels corresponded to reduced PD-L1 expression on MOC2 tumor cells similar to the response observed in MOC1, variable PD-L1 expression alteration in the other cellular subsets, including increased expression in endothelial cells, suggests the possibility of IFNβ-dependent or IFN-independent alterations in PD-L1 expression after targeted MEK and mTOR inhibition in MOC2 cancer and host cell subsets.

Author Manuscript Author Manuscript Author Manuscript Author Manuscript

DISCUSSION

Multiple different subsets of cells within the solid tumor microenvironment may express PD-L1/2, including tumor cells, vascular endothelial cells, cancer-associated fibroblasts, and a number of infiltrating immune cells, including myeloid-derived suppressor cells, mature macrophages, and Tregs.[18] Within stromal and infiltrating immune cells subsets, PD-L1/2 expression represents one mechanism of immune suppression leading to immune escape in the setting of an otherwise activated local antigen-specific antitumor immune response. In this study, we evaluated baseline and inducible PD-L1/2 expression on MOC cells in vitro as well as on several cell types within the complex tumor microenvironment. Our data indicate that not only is PD-L1 expressed on many different pools of cells within the tumor, but also that PD-L1 expression changes after treatment with agents targeting pro-growth and pro-survival signaling pathways in a complex manner that may be related in part to overall changes in tumor microenvironment IFN levels.

Links between deregulated cancer-promoting pro-growth and pro-survival signaling pathways and the development of a tumor-permissive microenvironment have been identified. Cancer cells often express suppressive cytokines, such as vascular endothelial growth factor, IL-10, and transforming growth factor-β downstream of signaling pathways activated by driver mutations.[19] Inhibition of upstream kinase receptors or downstream signaling through the PI3K and MAPK pathways via pharmacologic or genetic means variably reduces PD-L1 expression in different cancer cell lines, indicating that some tumors may acquire the ability to express PD-L1/2 autonomously.[10,20] Yet, strong correlations exist between tumor PD-L1 expression and infiltrating lymphocytes with geographic colocalization of PD-L1 and tumor-infiltrating lymphocytes, which is a common finding in tumor biopsies.[4,6,21] Taube et al[4] further associated this PD-L1 expression and TIL presence with local production of IFNγ; a finding later mechanistically and functionally validated.[2,22] Thus, although emerging evidence suggests that cell-autonomous expression of PD-L occurs secondary to oncogenic signaling in some tumor types and subsets, the majority of tumor cell PD-L1 expression is likely induced by IFNγ produced by nearby infiltrating immune cells in the setting of an activated adaptive immune response consistent with the concept of adaptive immune resistance.

Several lines of evidence support that PD-L1 expression is regulated by exogenous IFNγ as opposed to activation of oncogenic signaling pathways in MOC tumors. First, MOC cells harbor activating codon 61 *Ras* mutation (consistent with dimethylbenz[a]anthracene-induced carcinogenesis) leading to constitutively active MAPK signaling and coactivated PI3K/mTOR signaling, and are dependent upon activation of these signaling pathways for growth and survival in vivo (results not published). MOC1 and 2 PD-L1 expressions at baseline were very low, and neither mTOR nor MEK inhibition reduced this low baseline PD-L1 expression in either cell line. Rather, MEK inhibition increased PD-L1 expression in both, potentially because of cell stress as MEK inhibition, is cytotoxic to MOC cells. Thus, PD-L1 expression in MOC cells does not seem to be directly influenced by the oncogenic signaling pathways that drive their malignant potential. Second, PD-L1 expression and tumor IFNγ levels correlated at baseline and with changes after targeted therapy in IFNγ-high MOC1 tumors. MOC2 tumor cell PD-L1 expression, although very low at baseline,

Author Manuscript Author Manuscript Author Manuscript Author Manuscript

significantly decreased along with IFNγ levels as well. Conversely, endothelial and hematopoietic cells in the MOC tumor environment demonstrated variable changes in PD-L1 expression after targeted mTOR and MEK inhibition that seems to be cell-type dependent. Because these changes did not follow the pattern of tumor IFN changes, PD-L1 expression in these cells seem to be induced by IFN-independent inflammatory signals. Because changes in these cells seemed to be tightly linked to MEK inhibition as well, a direct effect of the MEK inhibitor on these cells cannot be ruled out.

The reduction of IFNγ levels in immunogenic MOC1 tumors after MEK but not mTOR inhibition is interesting. Although rapamycin is traditionally considered immunosuppressive, given its role in preventing solid organ transplant rejection, a growing body of evidence demonstrates antitumor activity with single agent rapamycin in a variety of tumor types, including HNSCC.[23] The MAPK pathway is critical for T-cell development and function, and recent evidence suggests that MEK inhibitors can induce transient but potent suppression of T-cell proliferation and cytokine production.[24] These data have significant implications for the rational combination of targeted and immunotherapies, and our laboratory is currently investigating the effect of a number of different targeted therapies on T-cell function to better inform this decision.

The exclusive dependence upon IFN for induction of PD-L1 expression in vitro in MOC1 and MOC2 tumor cells differs from the findings of others. Lu et al[25] demonstrated that, in addition to IFNγ, the inflammatory cytokines IL-1, IL-6, and tumor necrosis factor-α also induce PD-L1 in a synergistic fashion on Tca8113 human oral cancer cells. Further, common-gamma chain cytokines (IL-2, IL-7, and IL-15) directly induce expression of PD-L1 on T cells and indirectly on myeloid cells, and IL-6 and IL-10 induce PD-L1 in dendritic cells via a signal transducer and activator of transcription 3-dependent mechanism.[26,27] These data, combined with ours, suggest that the microenvironment cues responsible for PD-L1 expression may be cell-type dependent and may even vary between specific tumor cell lineages. Conversely, our finding that PD-L1 represents the dominant PD-L expressed in the SCC tumor microenvironment has been observed by others.[19,28] This potentially has significant implications for PD-blocking mAb therapy, and may explain, in part, why clinical responses observed with PD-1 and PD-L1 mAb therapy are similar.[8,9] Although it is possible that cytokines other than those used in this study could induce PD-L2 expression, colocalization of PD-L2 with PD-L1 when present in tumor samples makes this less likely.[28]

Our characterization of PD-L1 in MOC tumors yielded individually noteworthy findings. First, our finding that PD-L1 expression on CD31(+) tumor endothelial cells increased after MEK inhibition. Others have documented expression of PD-L on endothelial cells,[19,29] but our study is the first to document such changes after systemic targeted therapy. This could have clinical implications as infiltrating T cells are likely to encounter endothelial cell PD-L1 during extravasation and could thereby be excluded from the tumor microenvironment. Additionally, previous studies have demonstrated IFN-responsive endothelial cell PD-L1 expression, but our data argue for IFN-independent PD-L1 expression on endothelial cells in MOC tumors. That PD-L1 expression may be increased in certain cell types after systemic therapy with a targeted agent provides further support for combining targeted with anti-PD mAb therapy. Second, our finding that MOC2 tumor infiltrating mature F4/80(+)

Author Manuscript Author Manuscript Author Manuscript Author Manuscript

macrophages express dramatically elevated levels of PD-L1 despite being in an IFNγ-low microenvironment. This finding has been observed in other SCC models.[30] This suggests IFNγ-independent expression of PD-L1 on MOC2 tumor infiltrating macrophages, whereas PD-L1 expression did change with MEK inhibition and reduction of IFNγ in MOC1 macrophages. MOC1 tumor infiltrating macrophages are primarily of M1 phenotype, whereas the majority of MOC2 infiltrating macrophages are M2 (results not published). This suggests that phenotypically programmed M1 and M2 macrophages may differ in mechanism of PD-L1 expression. Given recent observations that tumor infiltrating immune cell PD-L1 expression correlates with patient response to PD-blocking mAb therapy,[31] this finding warrants further study.

Several limitations of this study exist. First, as with any mouse model of cancer, findings here may not be entirely representative of what occurs in human cancers. Next, we used PCR to measure transcript levels of IFNβ and IFNγ in MOC1 and MOC2 tumors, which allows us to only make relative assessments of cytokine levels. As such, some observed changes in cytokine levels that are relatively lower at baseline are difficult to interpret. An approach to measure absolute protein levels would have been to use an enzyme-linked immunosorbent assay-based assay to measure IFNβ than IFNγ in tumor lysate. Additionally, evaluation of changes in other proinflammatory cytokines in vivo, such as those that did not seem to induce PD-L1 expression on MOC tumor cells in vitro, may have provided a potential mechanism for changes in PD-L1 expression that were observed in the endothelial and hematopoietic cell subsets. Further, we did not exhaustively evaluate all subsets of cells that likely express PD-L1, and, as such, may have an incomplete picture of total tumor PD-L1 changes after targeted therapy. Dendritic cells, other CD4(+) T cells, CD8(+) T cells, and B cells all may express PD-L1 and contribute to the overall balance between antigen-specific cytotoxic T lymphocyte activation and suppression in the tumor microenvironment.

In conclusion, we have demonstrated that multiple pools of PD-L1 exist within the syngeneic MOC tumor microenvironment and that expression of PD-L1 on tumor cells seem to be tightly coupled to the presence of IFNγ both in vitro and in vivo. Conversely, expression of PD-L1 on endothelial and immune cells within the tumor microenvironment seems to be regulated, at least in part, by IFNβ-dependent or IFN-independent factors. Our findings of significantly elevated PD-L1 on macrophages and endothelial cells supports the findings of others, and warrants further investigation given the correlation between response to PD-blocking mAb therapy and PD-L1 expression on stromal and infiltrating immune cells. Interestingly, MEK, but not mTOR, inhibition reduced IFNγ levels in immunogenic MOC1 tumors, raising the possibility of immunosuppression. Importantly, high baseline PD-L1 expression coupled with high baseline IFNγ levels in immunogenic MOC1 tumors along with low baseline PD-L1 and IFNγ in poorly immunogenic MOC2 tumors validates this model as a powerful tool to study the effects of PD-blocking mAb therapies alone or in combination with small molecule inhibitor therapies, and this work is currently underway.

Author Manuscript Author Manuscript Author Manuscript Author Manuscript

Contract grant sponsor:

This work was supported by the Intramural Program of NIDCD. H.C. was supported through the National Institutes of Health (NIH) Medical Research Scholars Program, a public-private partnership supported jointly by the NIH and generous contributions to the Foundation for the NIH from Pfizer, The Doris Duke Charitable Foundation, The Newport Foundation, The American Association for Dental Research, The Howard Hughes Medical Institute, and the Colgate–Palmolive Company, as well as other private donors.

REFERENCES

1. Gajewski TF, Schreiber H, Fu YX. Innate and adaptive immune cells in the tumor microenvironment. Nat Immunol 2013;14:1014–1022. [PubMed: 24048123]
2. Spranger S, Spaapen RM, Zha Y, et al. Up-regulation of PD-L1, IDO, and T(regs) in the melanoma tumor microenvironment is driven by CD8(+) T cells. Sci Transl Med 2013;5:200ra116.
3. Tumeh PC, Harview CL, Yearley JH, et al. PD-1 blockade induces responses by inhibiting adaptive immune resistance. Nature 2014;515:568–571. [PubMed: 25428505]
4. Taube JM, Anders RA, Young GD, et al. Colocalization of inflammatory response with B7–h1 expression in human melanocytic lesions supports an adaptive resistance mechanism of immune escape. Sci Transl Med 2012;4: 127ra37.
5. Ward MJ, Thirdborough SM, Mellows T, et al. Tumour-infiltrating lymphocytes predict for outcome in HPV-positive oropharyngeal cancer. Br J Cancer 2014;110:489–500. [PubMed: 24169344]
6. Seiwert TY. A phase Ib study of MK-3475 in patients with human papillomavirus (HPV)-associated and non-HPV-associated head and neck (H/N) cancer. Head and Neck Cancer 2014 ASCO Annual Meeting. Abstract #6011.
7. Keck MK, Zuo Z, Khattri A, et al. Integrative analysis of head and neck cancer identifies two biologically distinct HPV and three non-HPV subtypes. Clin Cancer Res 2015;21:870–881. [PubMed: 25492084]
8. Topalian SL, Hodi FS, Brahmer JR, et al. Safety, activity, and immune correlates of anti-PD-1 antibody in cancer. N Engl J Med 2012;366:2443–2454. [PubMed: 22658127]
9. Brahmer JR, Tykodi SS, Chow LQ, et al. Safety and activity of anti-PD-L1 antibody in patients with advanced cancer. N Engl J Med 2012;366:2455–2465. [PubMed: 22658128]
10. Akbay EA, Koyama S, Carretero J, et al. Activation of the PD-1 pathway contributes to immune escape in EGFR-driven lung tumors. Cancer Discov 2013;3:1355–1363. [PubMed: 24078774]
11. Cancer Genome Atlas Network. Comprehensive genomic characterization of head and neck squamous cell carcinomas. Nature 2015;517:576–582. [PubMed: 25631445]
12. Vander Broek R, Mohan S, Eytan DF, Chen Z, Van Waes C. The PI3K/Akt/mTOR axis in head and neck cancer: functions, aberrations, crosstalk, and therapies. Oral Dis 2015;21:815–825. [PubMed: 24219320]
13. Judd NP, Winkler AE, Murillo–Sauca O, et al. ERK1/2 regulation of CD44 modulates oral cancer aggressiveness. Cancer Res 2012;72:365–374. [PubMed: 22086849]
14. Judd NP, Allen CT, Winkler AE, Uppaluri R. Comparative analysis of tumor-infiltrating lymphocytes in a syngeneic mouse model of oral cancer. Otolaryngol Head Neck Surg 2012;147:493–500. [PubMed: 22434099]
15. Onken MD, Winkler AE, Kanchi KL, et al. A surprising cross-species conservation in the genomic landscape of mouse and human oral cancer identifies a transcriptional signature predicting metastatic disease. Clin Cancer Res 2014;20:2873–2884. [PubMed: 24668645]
16. Guba M, Koehl GE, Neppl E, et al. Dosing of rapamycin is critical to achieve an optimal antiangiogenic effect against cancer. Transpl Int 2005; 18:89–94. [PubMed: 15612989]
17. Jessen WJ, Miller SJ, Jousma E, et al. MEK inhibition exhibits efficacy in human and mouse neurofibromatosis tumors. J Clin Invest 2013;123:340–347. [PubMed: 23221341]
18. Francisco LM, Sage PT, Sharpe AH. The PD-1 pathway in tolerance and autoimmunity. Immunol Rev 2010;236:219–242. [PubMed: 20636820]
19. Lippitz BE. Cytokine patterns in patients with cancer: a systematic review. Lancet Oncol 2013;14:e218–e228. [PubMed: 23639322]

Author Manuscript Author Manuscript Author Manuscript Author Manuscript

20. Atefi M, Avramis E, Lassen A, et al. Effects of MAPK and PI3K pathways on PD-L1 expression in melanoma. Clin Cancer Res 2014;20:3446–3457. [PubMed: 24812408]
21. Wimberly H, Brown JR, Schalper K, et al. PD-L1 expression correlates with tumor-infiltrating lymphocytes and response to neoadjuvant chemotherapy in breast cancer. Cancer Immunol Res 2015;3:326–332. [PubMed: 25527356]
22. Dovedi SJ, Adlard AL, Lipowska–Bhalla G, et al. Acquired resistance to fractionated radiotherapy can be overcome by concurrent PD-L1 blockade. Cancer Res 2014;74:5458–5468. [PubMed: 25274032]
23. Amornphimoltham P, Patel V, Sodhi A, et al. Mammalian target of rapamycin, a molecular target in squamous cell carcinomas of the head and neck. Cancer Res 2005;65:9953–9961. [PubMed: 16267020]
24. Liu L, Mayes PA, Eastman S, et al. The BRAF and MEK inhibitors dabrafenib and trametinib: effects on immune function and in combination with immunomodulatory antibodies targeting PD1, PD-L1, and CTLA-4. Clin Cancer Res 2015;21:1639–1651. [PubMed: 25589619]
25. Lu W, Lu L, Feng Y, et al. Inflammation promotes oral squamous carcinoma immune evasion via induced programmed death ligand-1 surface expression. Oncol Lett 2013;5:1519–1526. [PubMed: 23761816]
26. Kinter AL, Godbout EJ, McNally JP, et al. The common gamma-chain cytokines IL-2, IL-7, IL-15, and IL-21 induce the expression of programmed death-1 and its ligands. J Immunol 2008;181:6738–6746. [PubMed: 18981091]
27. Wölfle SJ, Strebovsky J, Bartz H, et al. PD-L1 expression on tolerogenic APCs is controlled by STAT-3. Eur J Immunol 2011;41:413–424. [PubMed: 21268011]
28. Taube JM, Klein A, Brahmer JR, et al. Association of PD-1, PD-1 ligands, and other features of the tumor immune microenvironment with response to anti-PD-1 therapy. Clin Cancer Res 2014;20:5064–5074. [PubMed: 24714771]
29. Rodig N, Ryan T, Allen JA, et al. Endothelial expression of PD-L1 and PD-L2 down-regulates CD8+ T cell activation and cytolysis. Eur J Immunol 2003;33:3117–3126. [PubMed: 14579280]
30. Belai EB, de Oliveira CE, Gasparoto TH, et al. PD-1 blockage delays murine squamous cell carcinoma development. Carcinogenesis 2014;35: 424–431. [PubMed: 24031027]
31. Herbst RS, Soria JC, Kowanetz M, et al. Predictive correlates of response to the anti-PD-L1 antibody MPDL3280A in cancer patients. Nature 2014; 515:563–567. [PubMed: 25428504]

Author Manuscript Author Manuscript Author Manuscript Author Manuscript

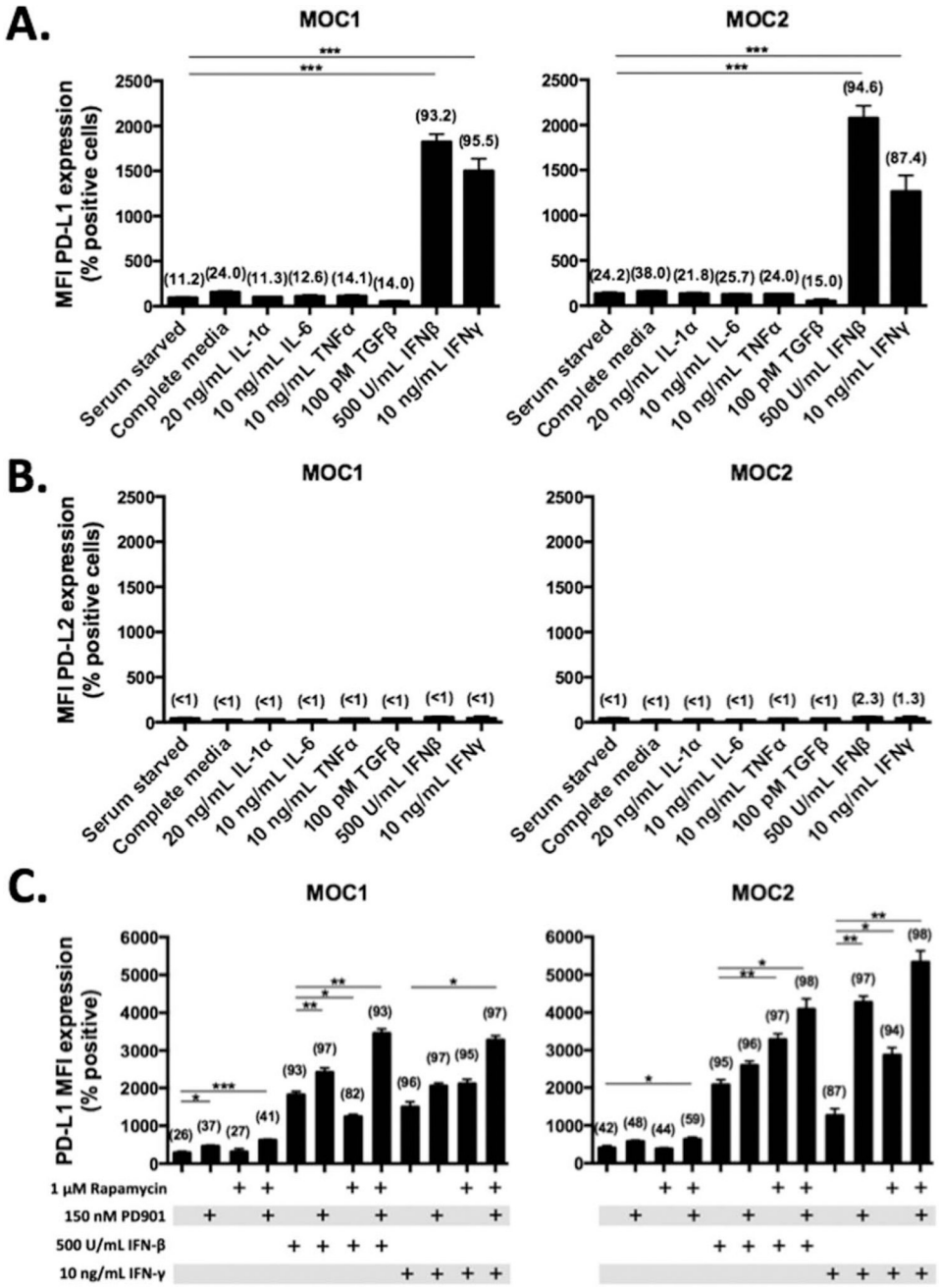

FIGURE 1.

Characterization of programmed death-ligand (PD-L) expression on murine oral cancer (MOC)1 and MOC2 cells. MOC1 and MOC2 cells were cultured in serum starved (24 hours) and growth factor or cytokine rich conditions as indicated and assessed for (A) PD-L1 and (B) PD-L2 expression via flow cytometry. Complete media includes 5% fetal calf serum (FCS), 5 ng/mL epidermal growth factor (EGF), and 5 ng/mL insulin. All cytokine stimulations were for 48 hours. Bar graphs represent mean mean fluorescence intensity (MFI) ± SEM with percent positive cells in parentheses. (C) MOC1 and MOC2 cells were treated in culture with rapamycin or PD901 for 48 hours in the presence or absence of

Author Manuscript Author Manuscript Author Manuscript Author Manuscript

interferon (IFN)β and IFNγ, as indicated. Bar graphs represent mean MFI ± SEM with percent positive cells in parentheses. All in vitro experiments were replicated at least once to ensure reproducibility. *$p < .05$; **$p < .01$; ***$p < .001$.

Author Manuscript Author Manuscript Author Manuscript Author Manuscript

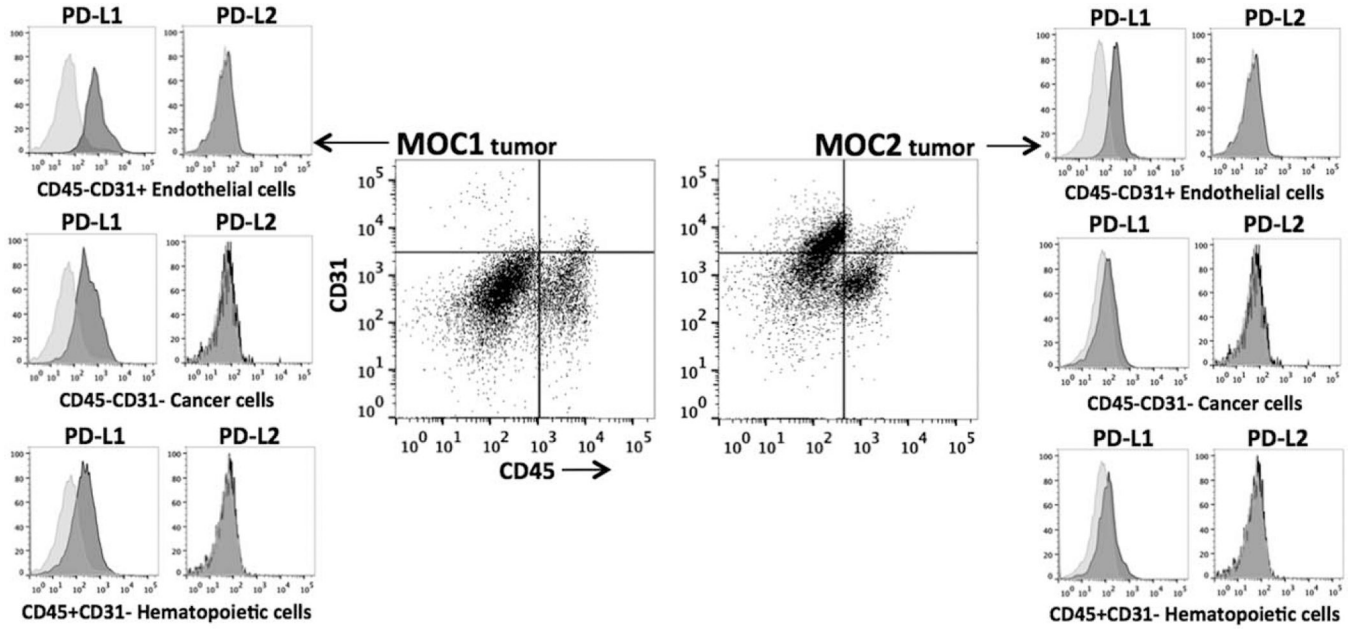

FIGURE 2.

Characterization of in vivo programmed death-ligand (PD-L) expression in murine oral cancer (MOC)1 and MOC2 tumors. Gating strategy for MOC tumors began with generation of a single cell suspension and exclusion of dead cells with 7AAD staining. Separation of cell subsets was accomplished by plotting CD45.2 against CD31. CD45(+)/CD31(−) cells were defined as infiltrating hematopoietic cells, CD31(+)/CD45(−) cells were defined as endothelial cells, and CD45(−)/CD31(−) cells were defined as tumor cells. Platelet-derived growth factor receptor (CD140a) staining on CD45(−)/CD31(−) cells indicated a low density of cancer-associated fibroblasts (<5%; data not shown). Histograms of PD-L1 and PD-L2 expression (dark shaded) from each cell subset are shown in relation to isotype control staining (light shaded) and are representative of day 50 MOC1 tumors ($n = 4$) and day 35 MOC2 tumors ($n = 7$).

Author Manuscript Author Manuscript Author Manuscript Author Manuscript

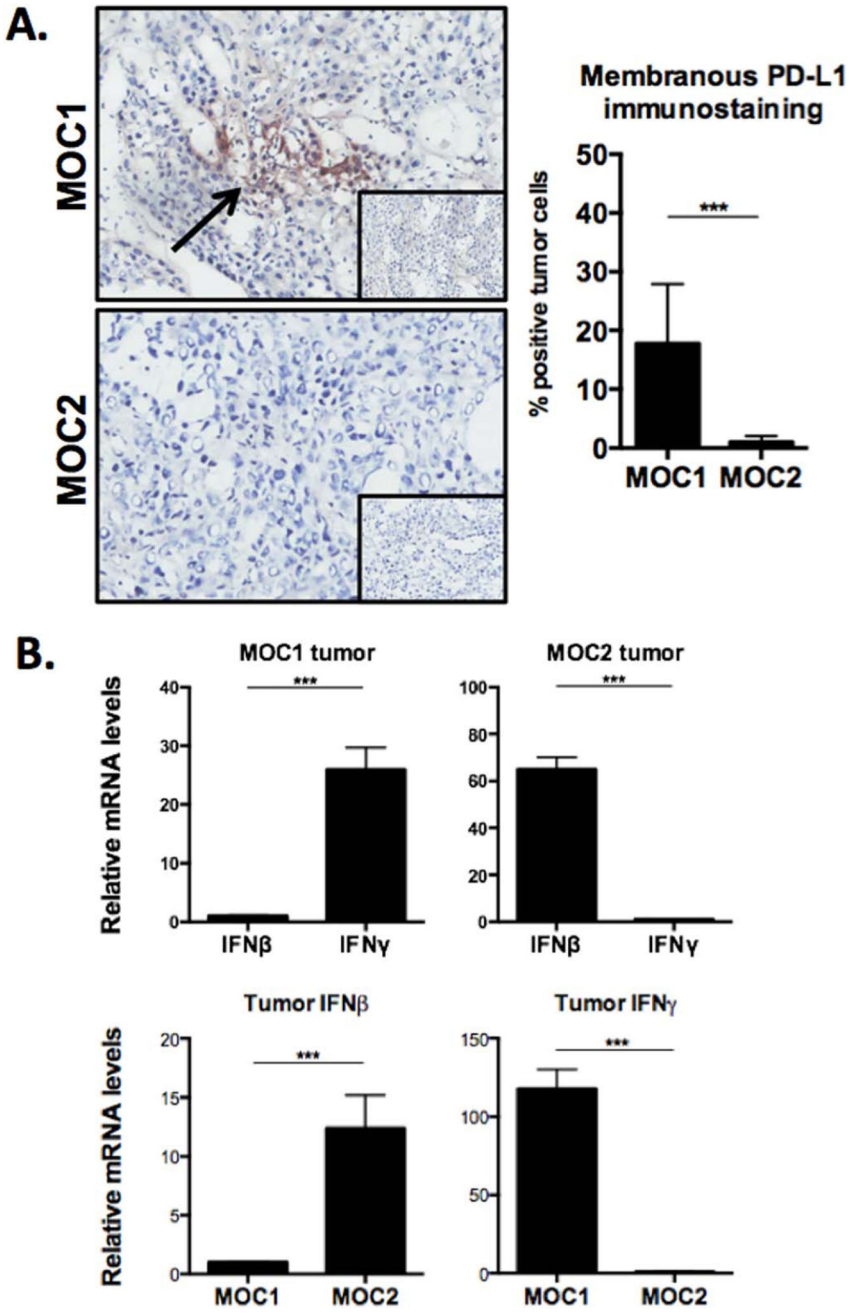

FIGURE 3.

Programmed death-ligand (PD-L)1 immunohistochemistry and interferon levels within murine oral cancer (MOC)1 and MOC2 tumors. (A) Immunohistochemical analysis of PD-L1 expression on fresh frozen MOC1 and MOC2 tumors, using the same antibody clone as was used in the flow cytometry experiments (clone 10F.9G2), demonstrated elevated PD-L1 expression in MOC1 consistent with flow cytometry results. Isotype control photomicrographs are inset (original magnification ×40). Percentage-positive cells averaged from 8 original magnification ×40 photomicrographs of regions of viable tumor. (B) Transcript levels of interferon (IFN)β and IFNγ were measured using real-time polymerase

Author Manuscript Author Manuscript Author Manuscript Author Manuscript

chain reaction (RT-PCR) from fresh tumor homogenates. For each comparison, the lower mean value was set to 1 and relative fold expression of the higher was assessed. Measurements are mean ± SEM of 3 separate tumors each assayed in technical triplicate. *$p < .05$; **$p < .01$; ***$p < .001$. [Color figure can be viewed in the online issue, which is available at wileyonlinelibrary.com.]

Author Manuscript
Author Manuscript
Author Manuscript
Author Manuscript

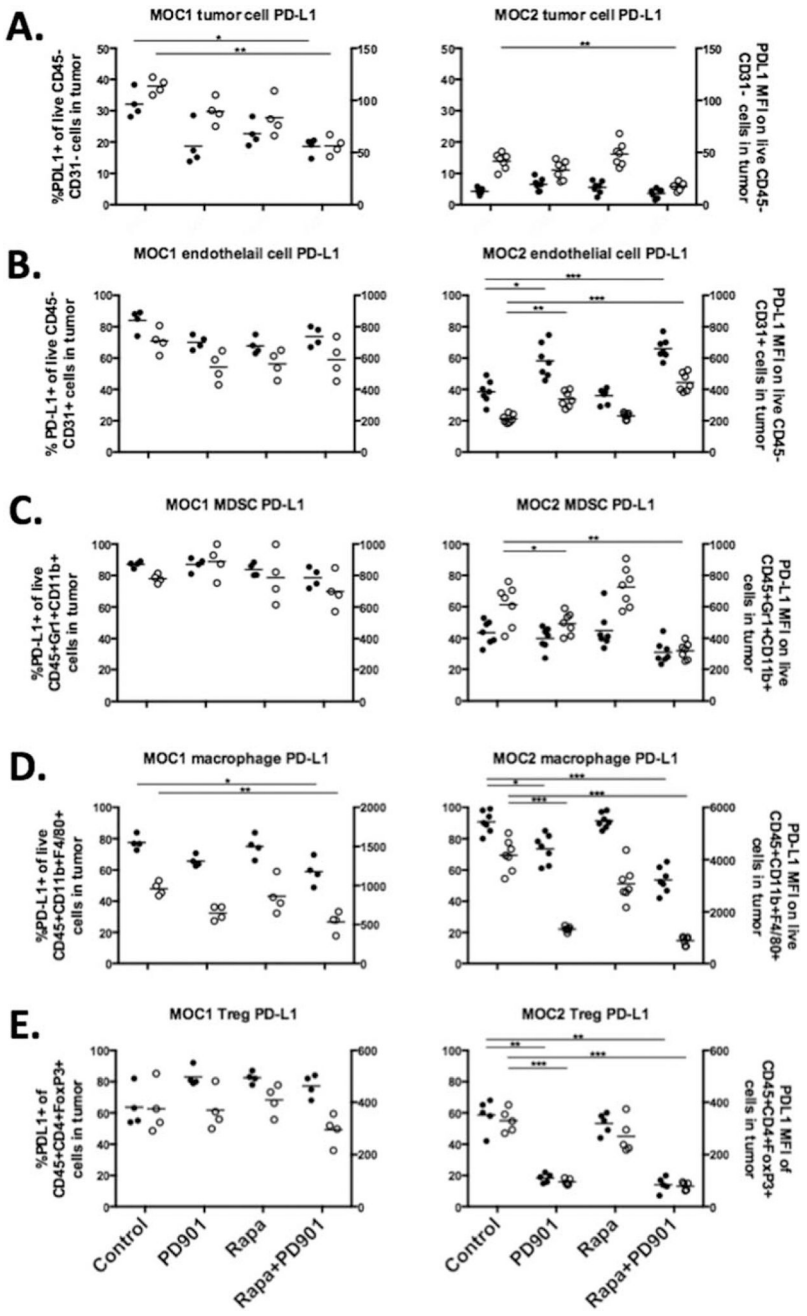

FIGURE 4.

Changes in programmed death-ligand (PD-L)1 expression on murine oral cancer (MOC)1 and MOC2 cell subsets after pharmacologic mammalian target of rapamycin (mTOR) and MEK inhibition in vivo. After 21 days of treatment in vivo with rapamycin (4.5 mg/kg i.p. loading dose then 1.5 mg/kgi.p. every other day) and PD901 (1.5 mg/kg oral gavage [OG] daily), CD45(−)/CD31(−) tumor cells (A), CD45(−)/CD31(+) endothelial cells (B), CD45(+)/CD11b(+)/Gr1(+) myeloid-derived suppressor cells (C), CD45(+)/CD11b(+)/F4/80(+) macrophages (D) and CD45(+)/CD3(+)/CD4(+)/FoxP3(+) regulatory T cells (Tregs) (E), were analyzed for PD-L1 expression in MOC1 ($n = 4$) and MOC2 ($n = 7$)

Author Manuscript Author Manuscript Author Manuscript Author Manuscript

tumors. For each plot, the left y-axis is the percentage of positive cells and represented by solid data points and the right y-axis is PD-L1 mean fluorescence intensity (MFI) and represented by hollow data points. Horizontal bars for each data set represent means. *$p < .05$; **$p < .01$; ***$p < .001$.

Author Manuscript Author Manuscript Author Manuscript Author Manuscript

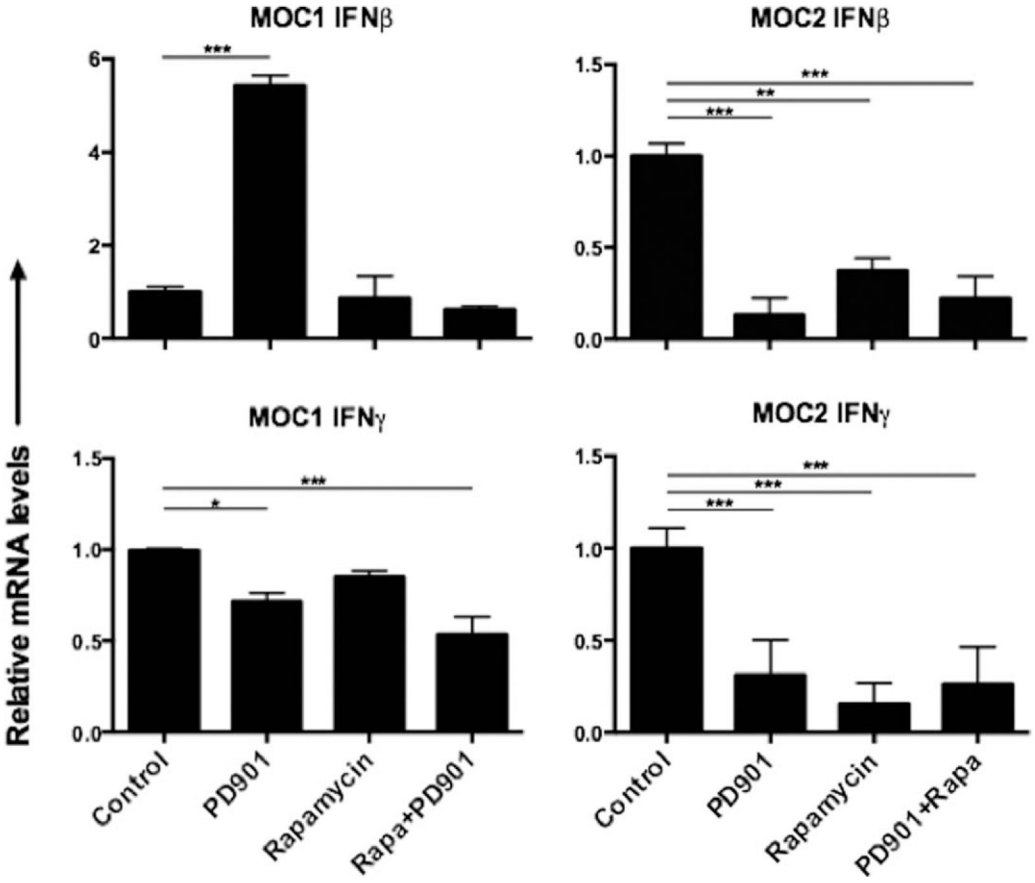

FIGURE 5.

Changes in tumor interferon levels after pharmacologic mammalian target of rapamycin (mTOR) and MEK inhibition. After treatment with rapamycin and PD901, as previously described, transcript levels of IFNβ and IFNγ were measured using real-time polymerase chain reaction (RT-PCR) from fresh tumor homogenates. For each analysis, the level of interferon (IFN) in untreated controls was set to 1 and relative changes in IFN levels with treatment were assessed. Measurements are mean ± SEM of 3 separate tumors each assayed in technical triplicate. *$p < .05$; **$p < .01$; ***$p < .001$.

Author Manuscript Author Manuscript Author Manuscript Author Manuscript

TABLE 1.

Baseline pools of programmed death-ligand-1 in murine oral cancer-1 and −2 tumors.

		M0C1 (*n* = 4)			M0C2 (*n* = 7)		
Cell type	**Markers to identify**	**% of cells in tumor**	**% PD-L1 positive**	**Mean PD-L1 MR**	**% of cells in tumor**	**% PD-L1 positive**	**Mean PD-L1 MFI**
Tumor cells	CD45(−)CD140a(−)CD31(−)	72 ± 5	32 ± 4	114 ± 7	45 ± 5 *	4 ± 1 *	42 ± 7 *
Endothelial cells	CD45(−)CD140a(−)CD31(+)	2 ± 0.5	84 ± 6	710 ± 78	25 ± 5 *	38 ± 7 *	213 ± 27 *
Hematopoietic cells	CD45(+)CD140a(−)CD31(−)	20 ± 3			20 ± 4		
Myeloid-derived suppressor cells	CD45(+)Gr1(+)CD11b(+)	5 ± 1	87 ± 2	781 ± 28	12 ± 1 *	44 ± 7 *	613 ± 128 **
Macrophages	CD45(+)CD11b(+)Ly6C^{low}F4/80(+)	5 ± 1	78 ± 5	960 ± 85	1 ± 0.5 *	91 ± 7 **	4167 ± 604 *
Tregs	CD45(+)CD4(+)FoxP3(+)	0.6 ± 0.2	64 ± 12	375 ± 97	2 ± 0.5 *	59 ± 10	330 ± 44

Abbreviations: MOC, murine oral cancer; PD-L, programmed death-ligand; MFI, mean fluorescence intensity; Tregs, regulatory T cells.

* $p < .01$;

** $p < .05$; significance in relation to corresponding measurements in MOC1 tumors.